A Water-Rich Cobalt(II) Compound: Hydrothermal Synthesis, Spectroscopic, Thermal, Crystal Structure Characterization and Antimicrobial Properties

Luann R. D'souza[a], Sanket K. Gaonkar[b], Sarvesh S. Harmalkar[a], Pratik A. Asogekar[a], Prof. Irene Furtado[b], Prof. Sunder N. Dhuri[a]*

[a] School of Chemical Sciences, Goa University, Taleigao Plateau, Goa, 403 206 India; *E-mail: sndhuri@unigoa.ac.in*
[b] Department of Microbiology, Goa University, Taleigao Plateau, Goa, 403 206 India

Dedicated to Professor Julio B. Fernandes on the occasion of his 68th birthday

Abstract

A water-rich mononuclear Co(II) compound, tris-(1,10-phenanthroline) cobalt(II) 1,4-phenylenediacrylate tetradecahydrate, $[Co(phen)_3](ppda)\cdot 14H_2O$ (**1**) (where phen is 1,10-phenanthroline; ppda is *p*-phenylenediacrylate) has been prepared and characterized by elemental analyses, IR, Raman, UV-Vis, fluorescence spectra, magnetic studies, cyclic voltammetry, single crystal X-ray diffractometry and TG-DTA. Co(II) ion in **1** is high spin (S = 3/2) with μ_B = ~ 3.98 B.M. and exhibits a reversible one electron Co^{II}/Co^{III} behavior in CV. It crystallizes in a monoclinic centrosymmetric *C*2/*c* space group with unit cell parameters; *a* = 23.1019(13), *b* = 12.1077(5) and *c* = 19.7428(1) Å; β = 111.410(2)°. The Co(II) ion is coordinated to three phen ligands forming the $[Co(phen)_3]^{2+}$ cation. $(ppda)^{2-}$ dianion and fourteen water molecules form a heterocyclic water cluster through O-H···O $(ppda)^{2-}$ and O-H···O (H_2O) interactions while phen ligands on adjacent cations are stacked via *π-π* interactions. Compound **1** loses its fourteen water molecules on heating upto 132 °C in TGA. Compound **1** is a potent inhibitor for Gram Negative E. coli as compared to Gram Positive S. aureus.

Introduction

The designing of smart molecules competent to function as sensors for molecular recognition of charged species is an ongoing challenge for researchers. The sensing of anions is an uphill battle due to its varied shapes, sizes, charges, high solvation energy, low charge densities, and pH sensitivity when compared to cationic species.[1-4] This has invoked an increasingly active search on developing efficient anionic species that can bind to the receptor's molecules *via* hydrogen bond donating groups. The characteristics possessed by an anion receptor are; a positively charged component for effective electrostatic interactions, hydrogen bond donor groups, and a stable framework for the assemblage of these anionic components. Hence, the anion receptor chemistry concerning the selective binding or sensing of negatively charged species is recognized to play a critical role in biology, medicine, catalysis.[1-10] Sharma and co-workers have reported some extensive work on tris-(phenanthroline)Co(III) cationic compounds such as $[Co(phen)_3](IO_4)_3\cdot 2H_2O$, $[Co(phen)_3](C_7H_4NSO_3)_3\cdot 8.5H_2O$, $[Co(phen)_3](BF_4)_3\cdot H_2O$, $[Co(phen)_3](PF_6)_3\cdot CH_3COCH_3$, $[Co(phen)_3](dnp)_3\cdot 4H_2O$, $[Co(phen)_3](Cl)[(CH_3)_3C_6H_2SO_3]_2\cdot 11H_2O$, and $[Co(phen)_3]_2[Hg(SCN)_4]_3\cdot 3H_2O$ behaving as anion receptors where $(IO_4)^-$, $(C_7H_4NSO_3)^-$, $(BF_4)^-$, $(PF_6)^-$, $(dnp)^-$, $((CH_3)_3C_6H_2SO_3)^-$ and $(SCN)^-$ are periodate, *o*-benzosulfimide, tetrafluoroborate, hexafluorophosphate, 2,4-dinitrophenolate, mesitylene sulphonate and thiocyanate respectively.[1-6] Apart from this, a lot of literature has been devoted to the $[Co(phen)_2(CO_3)]^+$ core which has garnered much interest in the context of anion recognition.[11-22] A very little attention has been paid towards Co(II) compounds in anion sensing, for instance; Geraghty and co-workers studied the role of $[Co(phen)_3](oda)\cdot 14H_2O$ and $[Co(phen)_3](nda)\cdot 11.5H_2O$ (where $odaH_2$ and $ndaH_2$ are octanedioic and nonanedioic acids respectively), significant in inhibiting the growth of yeast C. albicans.[23] Building synthetic receptors to sequester anions is getting tougher and needs careful consideration of selective binding through topological complementarity and non-covalent interactions. The hydrogen bonding and π-π interactions play pivotal roles in anchoring the anions in the crystal lattice thereby controlling the packing or assembly of the resulting compound.[24,25]

Many metal ions are involved in functioning of biological processes of life with cobalt being an essential trace element. The cobalt-based complexes have shown potential applications as drug carriers in medicine, as antibacterial, antiviral, antifungal and antioxidant agent.[26] The treatment of infectious ailments is a challenging task with the outbreak of a number of infectious diseases and ever-increasing number of multi-drug resistant microbial pathogens. This however, demands a substantial medical attention towards manufacturing new classes of antimicrobial agents. The primary factors underlying antimicrobial activity of metal complexes are denticity of ligands (example, bidentate ligands are influential than monodentate due to the chelate effect), the charge on the complex (cationic complexes are more efficient than neutral and anionic complexes), nuclearity (dinuclear complexes are more active than mononuclear ones)[27,28] 1,10-phenanthroline (phen) is a heterocyclic organic compound, known to exhibit exceptional *in vitro* antimicrobial activity against several bacterial and fungal pathogens. On account of being an avaricious chelating agent to a wide range of metals, the metal compounds of phen manifest potential in evoking cytotoxicity towards diseases and infections caused by cancer, viruses, bacteria and fungi. Hence, synthetic metal chelators such as phen have been accepted as therapeutic agents due to their ability to alter metabolism and homeostasis of microorganisms.[27] Taking into accord to fulfill the massive call for drugs to treat diseases, we sort to prepare the $[Co(phen)_3]^{2+}$ core and investigate its potential as an anion receptor for *p*-phenylenediacrylate dianion. To the best of our knowledge, there is no explicit report on the literature citing utilization of $[Co(phen)_3]^{2+}$ as a binding agent for *p*-phenylenediacrylates employing the second sphere coordination. Our growing interest in the rigid *p*-phenylenediacrylate, lies on its ability to form coordination polymers with diverse architectures, promising role as photocatalysts in dye

degradation and the use of Na_2BDA (BDA-benzenediacrylate) and Li_2BDA as organic battery electrode materials with excellent initial coulombic efficiency.[29-31] With the surge in industrialization causing environmental degradation, there is an urgent need to sequester such anions by binding them to a tunable synthetic recognition system. Bearing these notions in mind, we embarked on the synthesis of a new Co(II) anion receptor, $[Co(phen)_3](ppda)\cdot 14H_2O$ **1** showing potential antimicrobial efficiency against bacterial and fungal pathogens.

Results and Discussion

Synthetic aspects and spectroscopic characterization

The air-stable pale yellow crystals of $[Co(phen)_3](ppda)\cdot 14H_2O$ (**1**) were obtained using slow evaporation (method I) and solvothermal conditions (method II) by reacting $Co(OAc)_2\cdot 4H_2O$ with disodium *p*-phenylenediacrylate (Na_2ppda) and 1,10-phenanthroline (phen) under 1:1:3 stoichiometry in aqueous-ethanol mixture (Scheme 1). The elemental analyses confirmed that the formulae of the crystals obtained by method I and method II were identical (See Experimental details in Supporting Information), and the yield of the reactions were nearly quantitative. Compound **1** is freely soluble in water, methanol, and dimethyl sulfoxide. The crystalline samples of **1** obtained by method I and II were characterized by elemental analysis, IR, Raman, UV-Vis, TG-DTA and Powder X-ray diffraction. The crystal structure of the compound obtained by method II is reported here, while the discussion on PXRD is discussed in the subsequent Section 3.5.

The IR and Raman spectroscopies were used to provide an insight view of the presence of functional moieties and water molecules in **1**. The overlaid IR and Raman spectra of **1** obtained from the solvothermal route recorded in the region 4000-400 cm^{-1} are depicted in Figure 1. A broad IR band centered between 3327-3092 cm^{-1} is assigned to the O-H vibration of the lattice water molecules and broadening of the band suggests the presence of extensive H-bonding between water molecules and neighbouring H-acceptors $(ppda)^{2-}$ anion in **1**. The band at ~3060 cm^{-1} suggests the presence of saturation due to the =C-H vibrations of the aromatic $(ppda)^{2-}$. The absence of a distinct sharp band at around 1696 cm^{-1} confirms presence of deprotonated dicarboxylate $(ppda)^{2-}$.[1-6,26, 32-34] The C=C vibrations are observed between 1600-1400 cm^{-1}, the symmetric and anti-symmetric vibrations of dicarboxylate (ν_{COO^-}) appear at 1570-1530 cm^{-1} and 1425-1392 cm^{-1} respectively. This indicates that the carboxylate moiety is not coordinated to the cobalt(II) center (*vide infra*) in compound **1**.[35,36]

The Raman spectrum of **1** shows C-C skeletal stretching of phen between 1300-1632 cm^{-1} while the ranges of 1057-1600 and 700-1200 cm^{-1} are attributed to the C-H in- plane and out-of-plane bending vibrations respectively. The C-C in-plane bending of phen is observed below 1000 cm^{-1} while that of the out-of-plane which usually appears at 700 cm^{-1} is shifted to 727 cm^{-1} on coordination to cobalt.[37] While, the symmetrical COO^- stretch of $(ppda)^{2-}$ appears as a sharp peak at around 1593 cm^{-1}. The IR of the sample obtained by method I was recorded and compared with the sample produced from method II (Figure S1). All the bands in the two IR spectra nearly matched suggesting that the crystalline products obtained in both methods were the same. The Raman spectra of both samples were also identical.

The UV-Vis spectrum of **1** obtained by both methods were recorded in methanol, three characteristic bands at 205, 227 and 265 nm were observed, which are attributed to the ligand-centered (LC) $\pi \rightarrow \pi^*$ or $n \rightarrow \pi^*$ transitions originating from the metal-bound phen and $(ppda)^{2-}$ chromophores (Figure S2).[36, 38-40]. A weak intensity band appearing as a shoulder at 315 nm could be assigned to the metal-ligand or ligand-ligand charge transfer. The origin of visible spectra for cobalt(II) compounds may be due to spin-orbit coupling, vibrational or low symmetry components, and contribution of these parameters leads to difficulties in the total spectral analyses of cobalt(II) complexes.[36,39]

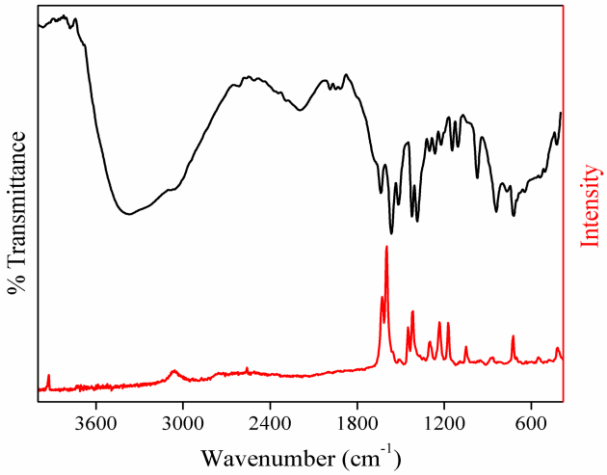

Figure 1. The combined solid-state IR and Raman spectra of compound **1** showing intense signals due to the organic moiety and lattice waters.

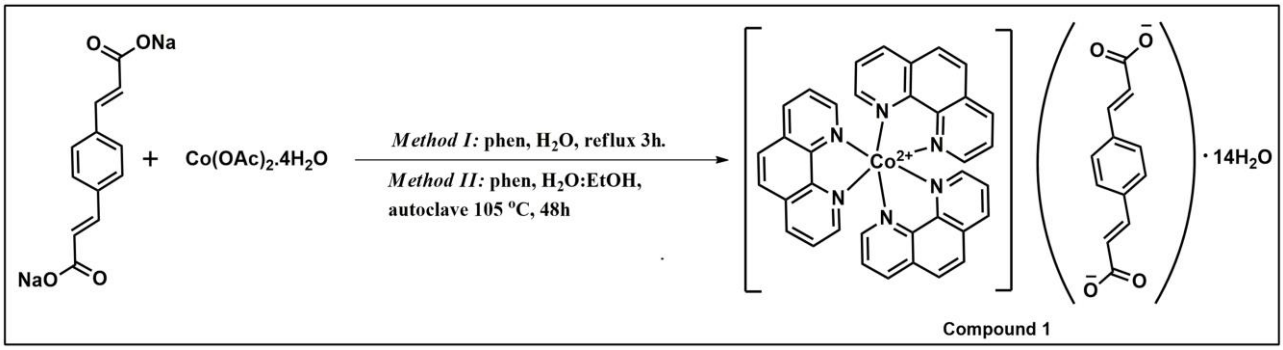

Scheme 1. Methods of preparation of the single crystals of $[Co(phen)_3](ppda)\cdot 14H_2O$ (**1**).

A broad absorption band observed in the region 420-550 nm with very low absorptivity is attributed to the $^4T_{1g}(F) \rightarrow {}^4T_{1g}(P)$ transition arising from the $3d^7$ cobalt(II) center (*vide infra*). [35,38,41-43]

The solid-state fluorescence emission spectrum of **1** obtained by both methods were recorded to understand emission properties of **1** at an excitation of 300 nm and were compared with the constituting free co-ligands H_2ppda and phen. The emission bands for H_2ppda appear at 407 and 430 nm which are attributed to the intra-ligand $\pi^* \rightarrow n$ or $\pi^* \rightarrow \pi$ energy transitions (Figure S3).[44-46] On other hand, phen which is known to be a weakly emissive compound, exhibits an emission peak at 425 nm with a shoulder centered at 481 nm arising from the closely lying $\pi \rightarrow \pi^*$ transitions of aromatic π -rings.[47-49] A weak emissive signal observed at 533 nm is assigned to the extended π-conjugation in the ligand system (phen).[50]The photoexcitation of **1** at 300 nm produces a luminescence spectrum showing resemblance to the phen spectrum with an emission maximum at 424 nm, a shoulder peak centering at 485 nm and a weak peak at 537 nm corresponding to ligand-centered (LC) fluorescence.[50] The emission bands of **1** show a decrease in luminescence intensity which is attributed to the coordination of phen to the Co(II) ion. The coordination of Co(II) to three phen ligands further cause expansion of the delocalized conjugation resulting in a red-shift with a decrease in efficiency of $\pi^* \rightarrow n$ transitions thereby decreasing the intensity of luminescence. It is well known that the structural property of any compound can have a profound effect on its luminescence.[51-53]

Magnetic and electrochemical investigations

The temperature dependent magnetic susceptibility (χ_M) measurements were performed on finely powdered sample of compound **1** under an applied magnetic field of 100 Oe in the temperature range of 60-310 K. The plot of χ_M *vs* T clearly depicts the influence of temperature on the Zero Field Cooled-Field Cooled (ZFC-FC) curves (Figure 2a). During the ZFC measurement, **1** was cooled to 60 K in the absence of applied field and thereafter studied with simultaneous heating up to 310 K in the presence of an external applied magnetic field. In the FC situation, initial cooling down to 60 K as well as heating back to 310 K was performed in the presence of an applied magnetic field. The magnetic susceptibility presented high values at 60 K which decreased on approaching room temperature. The FC-ZFC curves displayed an appreciable extent of bifurcation, higher χ_M values for FC measurements may be attributed to the spin alignment of the unpaired electrons with respect to the applied field (100 Oe) while in the case of ZFC, the lower observed χ_M values may be furnished to the randomization of the unpaired electron spins in the absence of an applied field.[54-60] Hence, the plot of variation of $\chi_M T$ with temperature revealed a typical paramagnetic behaviour (Figure 2b), which lies in accordance with the single crystal data discussed in the later section on crystallographic analysis (*vide infra*). The effective magnetic moment (μ_{eff}) at room temperature (298 K) was calculated from χ_M *vs* T plot and was found to be ~ 3.98 BM. The observed magnetic moment; thus, is in good agreement with the calculated spin only magnetic moment (μ_s = 3.87 B.M.) for high spin Co(II) with three unpaired electrons (S = 3/2). The slight increase observed in the value of μ_B could be due to the presence of minimal orbital angular momentum which is commonly perceived in Co(II) compounds. [59,60]

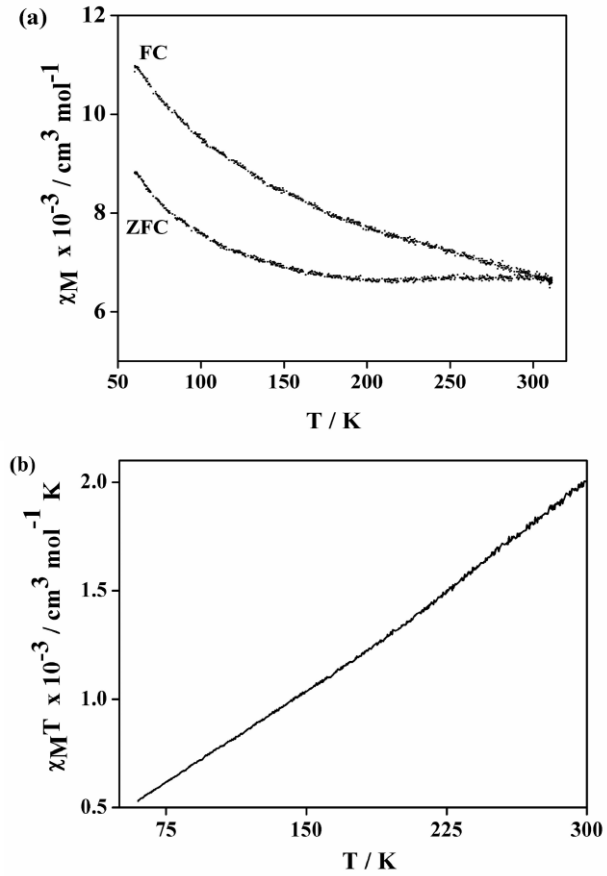

Figure 2. (a) Plot of Zero Field Cooled (ZFC) - Field Cooled (FC) magnetic susceptibility values as a function of temperature for **1** in an applied field of 100 Oe. (b) Plot of $\chi_M T$ vs T for **1**.

Cyclic voltammetry (CV) was used to understand the redox behavior of high spin cobalt(II) complex. The CV plot of **1** is shown in Figure 3. In the oxidation process, I_{pa} represents the anodic peak current having its anodic potential peak (E_{pa}) at 0.026 V *vs* Ag/AgCl reference electrode attributed to the oxidation of $[Co(phen)_3]^{2+}$ to $[Co(phen)_3]^{3+}$. On the other hand,

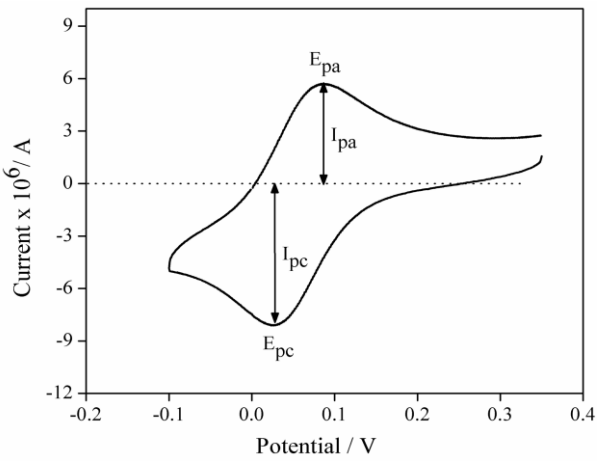

Figure 3. Cyclic voltammogram of **1** recorded at a scan rate of 100 mVs^{-1} in water containing 0.1 M KCl as supporting electrolyte against Ag/AgCl (saturated) reference electrode.

the reduction process is represented by the cathodic peak current (I_{pc}) which displays a cathodic potential peak (E_{pc}) at

0.086 V *vs* Ag/AgCl electrode attributed to the reverse step. The potential peak difference (ΔE) was calculated to be 0.059 V with an $E_{1/2}$ = 0.056 V. The redox potential (E^o) for the Co^{2+}/Co^{3+} couple was 0.137 V *vs* Ag/AgCl electrode which is in good agreement with the reported values of similar Co(II) compounds.[60-62] The CV plots of **1** were recorded at different scan rates (mV s^{-1}) in water containing 0.1 M KCl as the supporting electrolyte vs Ag/AgCl (sat. KCl) reference electrode. The CV data recorded at different scan rates were nearly identical and showed a proportional increase in the peak currents (Table S1 and Figure S4). The ΔE_p values at different scan rates clearly suggests the one electron reversible redox behavior of **1**.

Crystal structure description of compound 1

Compound **1** crystallizes in the monoclinic crystal system with a centrosymmetric *C2/c* space group, consisting of the $[Co(phen)_3]^{2+}$ cation within the lattice framework provided by the *p*-phenylenediacrylate dianion $(ppda)^{2-}$ and fourteen solvate water molecules (Figure 4).

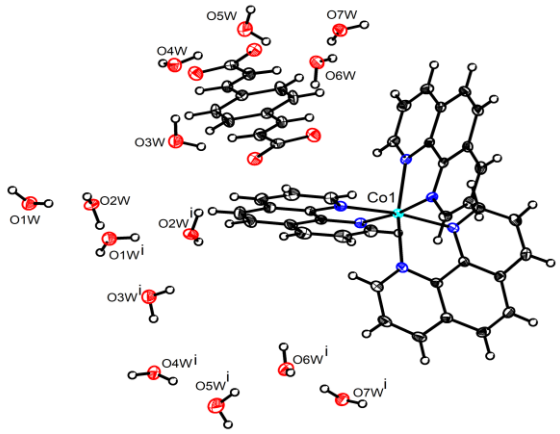

Figure 4. Crystal structure of $[Co(phen)_3]ppda{\cdot}14H_2O$ **1** showing $[Co(phen)_3]^{2+}$ cation and $(ppda)^{2-}$ anion with symmetry labels. Thermal ellipsoids are drawn at 50 % probability level for all the atoms excepting H atoms which are shown as spheres of arbitrary radii [i = -x + 1, y, -z + 3/2].

Crystal structure of **1** is composed of a crystallographically unique Co(II) core $½[Co(phen)_3]^{2+}$, half of the $(ppda)^{2-}$ dianion and seven water molecules. The remaining part of the cationic core, dianion and other seven water molecules are all symmetry generated (Figure S5). The crystal structure refinement details and selected bond distances along with bond angles for **1** are given in Table 1 and Table S2. The cationic core, $[Co(phen)_3]^{2+}$ is composed of the Co(II) ion bonded to three phen ligands resulting in a slightly distorted octahedral geometry (Figure S6). The Co-N bond distances and N-Co-N bond angles of **1** are compared with the Co-N bond distances and N-Co-N angles of some reported $[Co(phen)_3]^{2+}$ and $[Co(phen)_3]^{3+}$ compounds (Table S3).[20- 23,1-6] The Co-N bond lengths in reported Co(II)-phen compounds range from 2.127 to 2.147 Å while in those of Co(III)-phen compounds, the Co-N distances range from 1.934 to 1.942 Å (Table S3). In compound **1**, the Co-N bond distances range from 2.1208 to 2.1376 Å and are typical of Co(II)-phen compounds suggesting that in **1**, cobalt is in (+2) oxidation state and this data is in good agreement with our magnetic and CV results *(vide supra)*. In the crystal structure of **1**, there exist H-bonding interactions arising from the unison of O-H···O (water) and O-H···O $(ppda)^{2-}$ units (Table 2 and Figure S7).

Table 1. Selected structure refinement data of $[Co(phen)_3](ppda){\cdot}14H_2O$ (**1**)

Empirical formula	$C_{48}\ H_{60}\ Co\ N_6\ O_{18}$
Formula weight (g mol^{-1})	1067.95
Temperature (K)	100(2)
Wavelength (Å)	0.71073
Crystal system	Monoclinic
Space group	*C2/c*
Unit cell dimensions	
a (Å)	23.1091(13)
b(Å)	12.1077(5)
c (Å)	19.7428(10)
α = γ (°)	90
β (°)	111.410(2)
Volume ($Å^3$)	5142.8(4)
Z	4
Density (calc.) (mg/m^3)	1.379
Absorption coefficient (mm^{-1})	0.412
F(000)	2244
Crystal size (mm^3)	0.26 x 0.20 x 0.16
Theta range for data collection (°)	2.67 to 28.33
Completeness to theta	99.8%
Index ranges	-30≤ *h* ≤30 , -16 ≤ *k* ≤ 16 , -26 ≤ *l* ≤ 26
Reflections collected	38490
Independent reflections	6411 [R(int) = 0.0669]
Refinement method	Full-matrix least-squares on F^2
Absorption correction	Multi Scan
Data / restraints / parameters	6411 / 0 / 337
Goodness-of-fit on F^2	1.089
Final *R* indices [I>2sigma(I)]	R1 = 0.0551, wR2 = 0.1051
R indices (all data)	R1 = 0.0758, wR2 = 0.1141
Largest diff. peak and hole ($e.Å^{-3}$)	0.777 and -0.551

The assembly of $(ppda)^{2-}$ units and water molecules gives rise to a hetero water cluster network *via* hydrogen bonding interactions (pentagon bonding pattern) (Figure 5). The extensive hydrogen bonding network around either end of the $(ppda)^{2-}$ anions, defines a framework into which the cations are inserted (Figure S8). The complex cations form a layered network running in between $(ppda)^{2-}$ units prevailing due to *π-π* stacking interactions. The phen moiety attached to the Co(II) center is involved in *π-π* stacking interactions with phen moiety of the neighbouring cation with centroid-to-centroid distance

between the adjacent phen moieties close to 3.752 Å (Figure S9)[11,16,21,22,24,25], this features an offset or slipped stacking, i.e. the rings are parallely displaced, which is in accordance with the expected range for the reported phen-Co(II)/(III) compounds. Thus, the $(ppda)^{2-}$ dianion plays a complementary role in stabilizing the structure of **1** *via* hydrogen bonding, in addition to the *π- π* stacking interactions between the adjacent cationic units.

Table 2. Hydrogen bonding parameters (Å, °) for $[Co(phen)_3](ppda)\cdot 14H_2O$ (**1**)

D-H...A	d(D-H)	d(H...A)	<DHA	d(D...A)
O1w-H2···O4w^{ii}	0.850(0)	1.983(0)	165.16(0)	2.813(1)
O2w-H1 ···O7w^{iv}	0.850(1)	1.907(1)	175.39(0)	2.755(2)
O2w-H2···O1	0.850(1)	1.825(2)	173.69(0)	2.671(3)
O5w-H1···O6w^{iv}	0.850(0)	1.960(0)	164.95(0)	2.790(0)
O6w-H1···O2	0.850(1)	1.965(1)	165.04(0)	2.795(2)
O6w-H2···O3w	0.850(1)	1.880(2)	173.41(0)	2.726(3)
O7w-H1···O2w^{iii}	0.850(0)	1.974(0)	169.40(1)	2.814(0)
O7w-H2···O6w^{iv}	0.850(1)	1.953(2)	172.05(0)	2.797(2)
O3w-H1···O1	0.882(0)	1.878(0)	175.25(0)	2.757(1)
O4w-H2···O2	0.887(1)	1.825(2)	172.66(0)	2.707(3)
O4w-H1···O5w^{ii}	0.874(0)	1.870(0)	167.07(1)	2.729(0)
O1w-H1···O2w^{iii}	0.894(0)	1.920(1)	176.50(0)	2.813(1)
O3w-H2···O4w^{ii}	0.883(0)	2.049(1)	159.53(0)	2.893(2)
O5w-H2···O1w^{iii}	0.863(0)	1.914(1)	160.01(0)	2.742(1)

Note: The values in parentheses indicate estimated standard deviations. Symmetry codes: ii) -x + 3/2, y - 1/2, -z + 3/2, iii) x - 1/2, -y + 1/2, z – 1/2, iv) –x + 3/2, y+ 1/2, -z + 3/2.

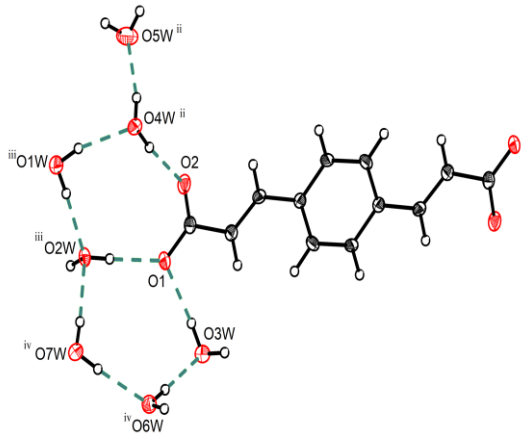

Figure 5. The hydrogen bonding interactions in **1** between the dianion $(ppda)^{2-}$ and the lattice water molecules giving rise to the formation of a pentagonal arrangement formed between carboxylate O-atoms (O1 and O2) and lattice water molecules (O4wii, O5wii, O1wiii, O2wiii, O6wiv and O7wiv). [ii) -x + 3/2, y - 1/2, -z + 3/2, iii) x - 1/2, -y + 1/2, z - 1/2, iv) -x + 3/2, y + 1/2, -z +

Thermogravimetric and differential temperature analysis (TG-DTA)

The thermal stability of compound **1** was investigated by TG-DTA techniques. From the TG plot, the first decomposition step occurs up to 132 ℃ with a weight loss of 24.5 % corresponding to complete dehydration of all fourteen lattice water molecules (*calcd*. 23.6 %) (Figure 6). The weight loss of water molecules is accompanied by two endothermic shoulders at ~ 100 ℃ in the DTA curve. The second thermal event takes place between 140-390 ℃ with decomposition of $(ppda)^{2-}$ moiety giving mass loss of 19.3 % (*calcd*. 20.2 %) accompanied by an endo peak at 285 ℃. The thermal decomposition above 400 ℃ results in the weight loss of 49.6 % corresponding to loss of three phen molecules (*calcd*. 50.6 %) and this TG event is accompanied by a sharp exotherm at 475 ℃ in the DTA curve. The final residue of 5.1 % remained after complete decomposition of **1** is of cobaltous(II) oxide. We also investigated TG-DTA of the sample obtained by method II. It was observed that both TG-DTA patterns obtained by method I and II were identical indicating the composition of **1** formed in two methods is the same.

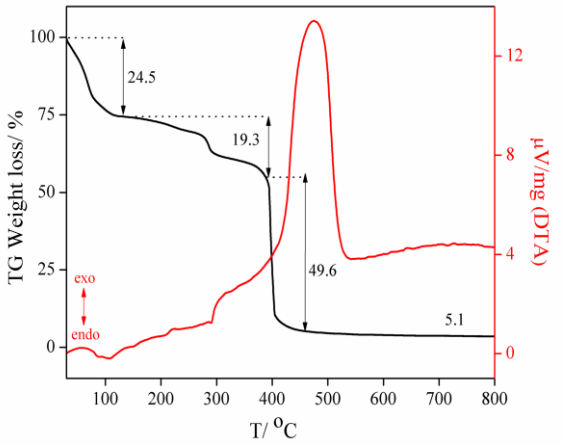

Figure 6. TG-DTA plot of compound **1** obtained by method I recorded in the temperature range 30-800 °C at a heating rate of 10°C /min in air atmosphere.

Antibacterial and Anti-Candida assays using Agar well diffusion method

Before testing compound **1** in biological studies, we have investigated the phase purity of **1** obtained by method I and II using X-ray powder diffraction technique. The X-ray powder patterns of the bulk samples of **1** obtained by method I and II were compared with their respective simulated X-ray powder patterns which were generated from single crystal data (Figure 7). As seen from Figure 7, the experimental and simulated X-ray powder patterns were nearly identical confirming phase purity of single crystals with the bulk samples of **1** obtained by the two methods. In order to check the stability of **1** in solution prior to microbial experiments, we characterized compound **1** by electrospray ionization mass spectrometry (ESI-MS) in CH_3OH solvent. The high resolution ESI-MS data of **1** exhibited three peaks at *m/z* = 181.0748, 209.5316 and 299.5606 peaks corresponding to $[Co(phen)(H_2O)_7]^{2+}$, $[Co(phen)_2]^{2+}$ and $[Co(phen)_3]^{2+}$ respectively (Figure S10). With confirmation of the

phase purity by PXRD and the stability of **1** in methanol, the powdered sample of **1** was then used in biological studies.

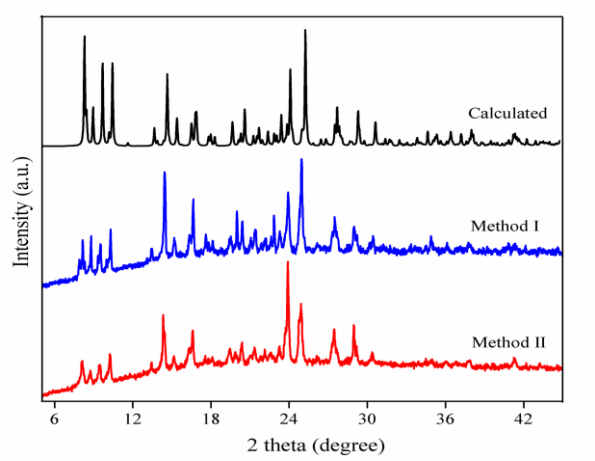

Figure 7. Comparison of experimental (red and blue) and calculated (black) PXRD patterns of **1**.

The antibacterial and anti-Candida activities of **1** were tested using the known agar well diffusion method[63] with bacterial cultures of *Escherichia coli* ATCC 8439 (Gram-Negative), *Staphylococcus aureus* (Gram-Positive) and the pathogenic yeast *C. albicans*. The degree of inhibition of growth with **1** for Gram-Negative *E. coli* was greater (34.8 ± 0.28 mm) than that of the Gram Positive *S. aureus* (32.5 ± 0.5 mm) and C. albicans (30 ± 0.5 mm) at 1.0 mg/mL level. On careful investigations, we observed that the zone of inhibition of growth of *E. coli, S. aureus* and *C. albicans* shown by **1**, were found to be two times (30 ± 0.5 to 34.8 ± 0.28 mm) sharper and clear than that shown by 1,10-phenanthroline (14.8 ± 0.76 to 18 ± 1 mm) (Figure 8). The absence of activity by *p*-phenylenediacrylic acid at the same concentration of 1.0 mg/mL revealed that it did not contribute effectively in killing the bacteria and yeast. The concomitant effect of *p*-phenylenediacrylic acid as a counter ion and 1,10-phenanthroline coordinated to cobalt(II) ion could be responsible for the enhancement in killing of these pathogens. The antimicrobial capability of phen is associated with its properties to chelate, inhibit the biological role of metal-dependent proteins, interfere with metal acquisition, bioavailability and metabolism for crucial reactions, disturbing the microbial cell homeostasis and culminating in the blockage of microbial nutrition, growth, development, cellular differentiation, adhesion to biotic and abiotic structures as well as featuring a salient role in *in vivo* progression. The action of metal complexes of phen inhibiting fungal pathogenic growth, takes place by damaging their mitochondrial function, uncoupling respiration, causing non-specific DNA cleavage, disrupting cell division and thereby inducing gross distortions in the fungal cell morphology.[27,28,64,65] The earlier published work by Geraghty and co-workers furnished the cobalt(II) complexes of octanedioic acid ($odaH_2$) and nonanedioic acid ($ndaH_2$) to exhibit greater anti-Candida activity in terms of % cell growth at 200 µg/mL than the uncomplexed acids, but however; reduced activity on comparison with 1,10-phenanthroline.[23]

The recent work by Gaëlle *et al*, showed that the pathogens such as *E. coli*, *P. aeruginosa*, *S. typhi*, *S. aureus* and *C. albicans* species namely *C. albicans ATCC 12C*, *C. albicans ATCC P37037*, *C. albicans ATCC P37039*, and *C. neoformans* are highly susceptible to cobalt(II) / (III) complexes

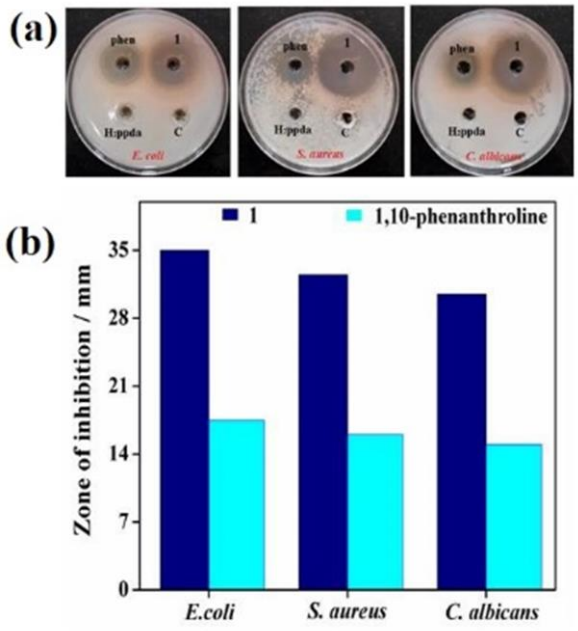

Figure 8. (a) Zone of inhibition of growth of *E. coli, S. aureus* and *C. albicans* by **1**, phen, H_2ppda and DMSO: H_2O (Control) at 1.0 mg/mL concentration level. (b) Histogram of inhibition zones of **1** and phen against the pathogenic bacterial and yeast species.

of 1,10-phenanthroline and co-ligands such as nitrate and azide at 2.0 mg/mL concentration.[33] Similar to our results, the coordination of these ligands to the metal ions have impacted the antibacterial and anti-Candida activity with growth inhibition zone diameters ranging between 13 to 38 mm. The reaction of metal ions with ligand plays a role in enhancing the antimicrobial effect by way of reducing the polarity of the metal ions by partial sharing of the positive charge with the donor atoms of the ligand (nitrogen atoms in case of phen) so as to favor electron delocalization in the metal complex. These properties often result in increasing the hydrophobic and lipophilic character of metal complexes enabling them to permeate through the lipid layer of the pathogen, thereby killing the pathogens more effectively. [33, 66-68]

Furthermore, the antimicrobial activities were evaluated by determining their minimum inhibitory concentration (MIC). The MIC indicates the lowest concentration of **1**, at which a visible inhibition growth of micro-organisms is observed. On testing the effect of different concentrations of **1** *viz*. at 20, 40, 60, 80, 100, 300, 500, 700, 900 µg/mL on the growth of *E. coli*, *S. aureus* and *C. albicans* in a dose dependent manner, it was observed that the growth inhibition zones varied in the range of 21.0 - 28.1 mm for *E. coli*, 20.0 - 26.8 mm for *S. aureus* and 19.0 - 26.6 mm for *C. albicans* (Figure 9). In all the cases, the MIC was fixed at 100 µg/mL, as it is the lowest concentration at which no visible growth was seen. As reported by Gaëlle and co-workers, the MIC values for cobalt complexes obtained by the micro-broth dilution test were lower than those of a copper(II) complex against *E. coli*, *P. aeruginosa*, *S. typhi* and fungal species *C. albicans ATCC P37037* and *C. neoformans*.[33] The *in vitro* screening of $Co(phen)_3]Br_{1.5}Cl_{1.5}\cdot 6H_2O$ at 250 µg/disc exhibited good activity against the microbes *S. aureus*, *P. aerugenosa*, *V. parahaemolyticus* and *P. vulgaris*; with no detrimental effect on

E. coli.[36] Our results are of significance as S. aureus and C. albicans used in the study were clinical pathogens causing hospital acquired infections. Further, the synthesis of cobalt-phen compounds offers the researcher an opportunity to explore structural diversity of the complexes by controlling the geometry and varying the oxidation states of the metal centre. Secondly, with the inclusion of appropriate auxiliary ligand in the structure, it is expected to provide opportunities for targeting different biochemical pathways in bacteria causing their death. From our investigations, we thus conclude that tris(phenanthroline)Co(II) cation stabilized by *p*-phenylenediacrylate could be looked as the potential antimicrobial agent.

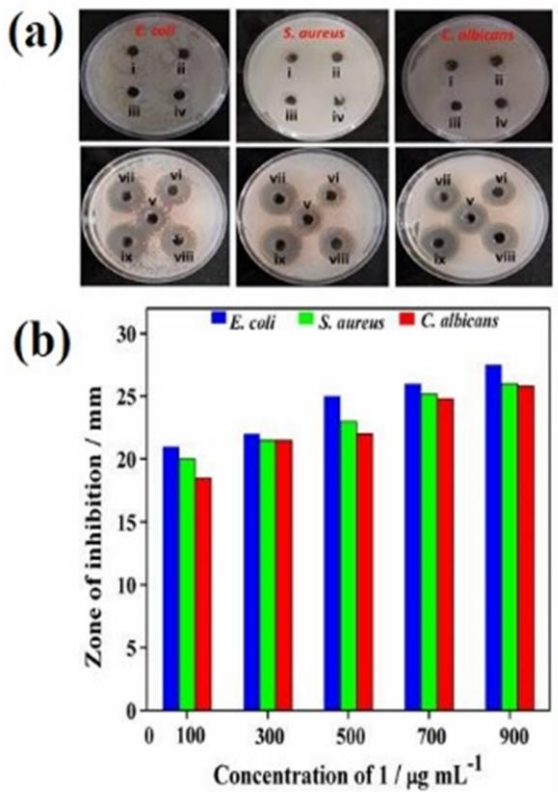

Figure 9. (a) Inhibition of growth of *E. coli*, *S. aureus* and *C*. albicans by **1** at different concentrations in μg/mL ; i) 20, ii) 40, iii) 60, iv) 80, v) 100, vi) 300, vii) 500, viii) 700 and ix) 900. (b) The histogram of inhibition zones of **1** against the pathogenic bacterial and fungal species at different concentrations in μg/mL; i) 20 ii) 40 iii) 60 iv) 80 v) 100 vi) 300 vii) 500 viii) 700 and ix) 900.

Conclusion

We have reported the synthesis of a new cobalt(II) water-rich compound, $[Co(phen)_3](ppda)\cdot 14H_2O$ (**1**) by slow evaporation and solvothermal methods in which cobalt(II) acetate, disodium salt of *p*-phenylenediacrylic acid and 1,10-phenanthroline were reacted in 1:1:3 stoichiometry. Compound **1** is fully characterized by several methods including single crystal X-ray diffraction technique which reveals an assembly of $(ppda)^{2-}$ anions and crystal water molecules forming a hetero water-cluster network through hydrogen bonding interactions (pentagon pattern). Compound **1** exhibited profound antimicrobial activity against *E. coli ATCC 8439*, and clinical strains *S. aureus* and *C. albicans* which suggests its plausible role as antibacterial and anti-Candida agents.

Deposition Number: CCDC 2017976 for (**1**), contain the supplementary crystallographic data for this paper. These data are provided free of charge by the joint Cambridge Crystallographic Data Centre and Fachinformationszentrum Karlsruhe Access Structures service www.ccdc.cam.ac.uk-/structures.

Supporting Information Summary

This experimental section, characterization and emission spectra are available in Supporting Information. The supplementary material file contains additional figures (Figure S1-S10) and tables (Table S1-S3). The crystal cif structure data and checkcif of compound **1** are given in supplementary material.

Acknowledgements

SND thanks the Council of Scientific and Industrial Research, New Delhi (No. 01(2923)/18/EMR-II) for financial support. Authors would like to thank Dr. Ruchi Gaur, Department of Chemistry, IIT Kanpur, Uttar Pradesh, India for extending help with Single Crystal X-ray data collection, and the Department of Microbiology, Goa Medical College, Goa, India for providing pathogenic bacterial and yeast cultures.

Conflict of interest

The authors declare no conflict of interest.

Keywords: Antimicrobial, Cobalt(II), Crystal structure, 1,10-Phenanthroline, 1,4-Phenylenediacrylic acid, Water-rich.

References

[1] R. P. Sharma, A. Singh, P. Brandão, V. Felix, P. Venugopalan, *J. Mol. Struct*. **2008**, *888*, 291-299.

[2] A. Singh, R. P. Sharma, P. Brandão, V. Felix, P. Venugopalan, *J. Mol. Struct.* **2008**, *891* 396-403.

[3] R. P. Sharma, A. Singh, P. Brandão, V. Felix, P. Venugopalan, J. Mol. Struct. **2009**, *920*, 119-127.

[4] R. P. Sharma, A. Singh, P. Brandão, V. Ferretti, P. Venugopalan, *J. Mol. Struct*. **2009**, *918*, 123-128.

[5] R. P. Sharma, A. Singh, P. Brandão, V. Felix, P. Venugopalan, *J. Mol. Struct*. **2009**, *918*, 1- 9.

[6] R. P. Sharma, A. Singh, P. Venugopalan, P. Brandão, V. Felix, *J. Mol. Struct*. **2009**, *933*, 63-68.

[7] P. A. Gale, S. E. Garcıa-Garrido, J. Garric, *Chem. Soc. Rev*. **2008**, *37*, 151-190.

[8] F. P. Schmidtchen, *Topics in Current Chemistry*, Springer-Verlag**, 2005**, *255*, 1-29.

[9] F. Davis, S. D. Collyer, S. P. J. Higson, *Topics in Current Chemistry*, Springer-Verlag**, 2005**, *255*, 97-124.

[10] P. D. Beer, S. R. Bayly, *Topics in Current Chemistry*, Springer-Verlag**, 2005**, *255*, 125-162.

[11] A. Singh, R. P. Sharma, T. Aree, P. Venugopalan, *CrystEngComm*. **2013**, *15*, 1153-1163.

[12] X. -C. Fu, X. -Y. Wang, M. -T. Li, C. -G. Wang, X. -T. Deng, *Acta Cryst*., **2006**, *E62*, 1263-1265.

[13] A. Singh, R. P. Sharma, T. Aree, P. Venugopalan, *J. Chem. Sci.* **2010**,*122*, 739-750.

[14] R. P. Sharma, A. Singh, P. Venugopalan, A. Rodríguez-Diéguez, J. M. Salas, *J. Mol. Struct*. **2013**, *1033*, 208-214.

[15] R. P. Sharma, A. Singh, P. Venugopalan, W. T. A. Harrison, *J. Mol. Struct*., **2011**, *994*, 6-12.

[16] R. P. Sharma, A. Singh, P. Brandão, V. Felix, P. Venugopalan, *J. Mol. Struct.* **2009**, *921*, 227-232.

[17] B. K. Koo, J. Kim, W. T. Lim, *J. Korean Chem. Soc*. **2007**, *51*, 595-599.

[18] E. C. Niederhoffer, A. E. Martell, P. Rudolf, A. Clearfield, *Inorg. Chem,* **1982**, *21*, 3734-3741.

[19] R. Seetharaj, P. V. Vandana, P. Arya, S. Mathew, *Arab. J. Chem*. **2019**,*12*, 295-315.

[20] D. Boys, C. Escobar, O. Wittke, *Acta Cryst*. **1984**, *C40*, 1359-1362.

[21] N. -P. Pook, P. Hentrich, M. Gjikaj, *Acta Cryst*. **2015**, *E71*, 910-914.

[22] D. J. Harding, P. Harding, Harry Adams, *Acta Cryst.* **2008**, *E64*, 1538-1538.

[23] M. Geraghty, M. McCann, M. Devereux, V. McKee, *Inorg. Chim. Acta*. **1999**, *293*, 160-166.

[24] C. Janiak, Dalton Trans. **2000**, *21*, 3885- 3896.

[25] C. R. Martinez, B. L. Iverson, *Chem. Sci*. **2012**, *3*, 2191- 2201.

[26] S. Arora, D. Talwar, M. Singh, S. C. Sahoo, R. Sharma, *J. Mol. Struct.* **2020**, *1199*, 127017.

[27] M. Rizzotto, *IntechOpen Chpt 5*, **2012**, 73.

[28] M. A. Zoroddu, S. Zanetti, R. Pogni, R. Basosi, *J. Inorg. Biochem*.**1996**, *63*, 291-300.

[29] Q. Sun, A. -L. Cheng, K. Wang, X-C. Yi, E-Q. Gao, *CrystEngComm*, **2015**, *17*, 1389-1397.

[30] X. -G. Sang, X. -X. Liu, *J. Coord. Chem*. **2014**, *67*, 2301-2311.

[31] V. A. Mihali, S. Renault, L. Nyholm, D. Brandell, *RSC Adv*. **2014**, *4*, 38004-38011.

[32] S. Jing, X. Jia- Ning, S. Tian- You, H. Xin, Y. Jun-Wei, W. Li, F. Yong, Z. Ping, *J. Coord. Chem.* **2007**, *60*, 295-300.

[33] D. S. Y. Gaëlle, D. M. Yufanyi, R. Jagan, M. O. Agwara, *Cogent Chemistry*, **2016**, *2*, 1-16.

[34] K. Nakamoto, Infrared and Raman spectra of Inorganic and coordination compounds part B: Applications in Coordination Compounds, Part-B Sixth Ed., John Wiley, **2009**.

[35] B. R. Srinivasan, S. C. Sawant, *Indian J. Chem*. *Sect. A*. **2004**, *43*, 1066-1075.

[36] K. A. Kumar, P. Meera, M. Amutha Selvi, A. Dayalan, *Int. J. Chem. Sci*. **2011**, *9*, 1421-1428.

[37] K. Krishnan, R. A. Plane, *J. Spectrochim. Acta A*, **1969**, *25*, 831-837.

[38] M. Garai, D. Dey, H. R. Yadav, M. Maji, A.R. Choudhury, B. Biswas, *J. Chem. Sci*. **2017**, *129*, 1513-1520.

[39] D. Avci, S. Altürk, F. Sönmez, Ö. Tamer, A. Başoğlu,Y. Atalay, B. Z. Kurt, N. Dege, *Appl Organometal Chem.* **2020**, *34*, 1-14.

[40] K. Yamasaki, T. Hara, M. Yasuda, *Proc. Jap. Acad*. **1953**, *29*, 337-341.

[41] S. Kundu, S. Roy, K. Bhar, R. Ghosh, R, C. -H. Lin, J. Ribas, B. K. Ghosh, *J. Chem. Sci*. **2013**, *125*, 723-730.

[42] S. Mistri, E. Zangrando, A. Figuerola, A. Adhikary, S. Konar, J. Cano, S. C. Manna, *Cryst.Growth Des*. **2014**, *14*, 3276-3285.

[43] C. -Q. Shen, T. -L. Yan, Y. -T. Wang, Z. -J. Ye, C. -J. Xu, W. -J. Zhou, *J. Lumin.* **2017**, *184*, 48-54.

[44] X. -H. Zhou, H. -H. Li, W. Huang, *Inorg. Chim. Acta.* **2012**, *384*, 184-188.

[45] Z. Su, J. Fan, M. Chen, T. –aki. Okamura, W. -Y. Sun, *Cryst.Growth Des*. **2011**, *11*, 1159-1169.

[46] C. Li, H. -C. Zhao, Y.-L. Zhu, Y.-H. Kan, K. -R. Ma, X. -M. Pan, *J. Iran Chem. Soc.* **2015**, *12*, 1227-1233.

[47] X.-M. Wang, R.-Q. Fan, L.-S. Qiang, P. Wang, Y.-L. Yang, Y.-L. Wang, *Inorg. Chem. Commun*. **2015**, *55*, 73-76.

[48] Z. -F. Wu, B. Tan, Z. -H. Deng, Z. -L. Xie, J. -J. Fu, N. -N. Shen, X.-Y. Huang, *Chem. Eur. J*. **2016**, *22*, 1334-1339.

[49] S. Goswami, S. Singha, R. Saha, A. S. Roy, M. Islam, S. Kumar, *Inorg. Chim. Acta*, **2018**, *486*, 353-360.

[50] Y. -Q. Huang, H. -Y. Chen, Z. -G. Li, Q. Wang, Y. Wang, X.-Q. Cao, Y. Zhao*, Inorg. Chim. Acta*, **2017**, *466*, 71-77.

[51] L. Ni, J. Wang, C. Liu, J. Fan, Y. Sun, Z. Zhou, G. Diao, *Inorg. Chem. Front.* **2016**, *3*, 959-968.

[52] Y. Yu, *J. Mol. Struct*. **2017**, *1149*, 761-765.

[53] R. Kumar, P. Bhargava, A. Dvivedi, *Procedia Mater. Sci*. **2015**, *10*, 37-43.

[54] A. Bayri, *Trans. Met. Chem*. **2005**, *30*, 987-991.

[55] S. G. Gawas, S. S. Meena, S. M. Yusuf, V. M. S. Verenkar, *New J. Chem.* **2016**, *40*, 9275-9284.

[56] P. A. Asogekar, V. M. S. Verenkar, *Ceramics Int.* **2019**, *45*, 21793-21803.

[57] S. Wöhlert, T. Runčevski, R. E. Dinnebier, S. G. Ebbinghaus, C. Näther, *Cryst.Growth Des.* **2014**, *14*, 1902-1913.

[58] J. Datta, A. Dey, S. K. Neogi, M. Das, S. Middya, R. Jana, S. Bandyopadhyay, A. Layek, P. P. Ray, *IEEE Trans. On Electron Devices*, **2017**, *64*, 4724-4730.

[59] H. Mao, C. Zhang, G. Li, H. Zhang, H. Hou, L. Li, Q. Wu, Y. Zhu, E. Wang, *Dalton Trans*. **2004**, *22*, 3918-3925.

[60] I. S. Y. Louise, S. Nabila, K. H. Sugiyarto, *Orient. J. Chem.* **2019**, *35*, 1500-1507.

[61] N. Elgrishi, K. J. Rountree, B. D. McCarthy, E. S. Rountree, T. T. Eisenhart, J. L. Dempsey, *J. Chem. Ed*. **2018**, *95*, 197-206.

[62] A. Congreve, R. Kataky, M. Knell, D. Parker, H. Puschmann, K. Senanayake, L. Wylie, *New J. Chem*. **2003**, *27*, 98-106.

[63] K. E. Cooper, A.H. Linton, S. N. Sehgal, *J. Gen. Microbiology*, **1958**, *18*, 670-687.

[64] L. Viganor, O. Howe, P. Mc Carron, M. McCann, M. Devereux, *Curr. Top. Med. Chem*. **2017**, *17*, 1280-1302.

[65] S. S. Harmalkar, R. J. Butcher, V. V. Gobre, S. K. Gaonkar, L. R. D'Souza, M. Sankaralingam, I. Furtado, S. N. Dhuri, *Inorg. Chim. Acta*, **2019**, *498*, 119020.

[66] C. Amah, A. M. Ondoh, D. M. Yufanyi, D. S. Y. Gaelle, *Internat. J. Chem.* **2015**, *7*, 10-20.

[67] Z. H. Chohan, A. Munawar, C. T. Supuran, *Met. Based Drugs*, **2001**, *8*, 137-143.

[68] C. Yenikaya, M. Poyraz, M. Sarı, F. Demirci, H. İlkimen, O. Büyükgüngör, *Polyhedron,* **2009**, *28*, 3526-3532.

A Water-Rich Cobalt(II) Compound: Hydrothermal Synthesis, Spectroscopic, Thermal, Crystal Structure Characterization and Antimicrobial Properties

Luann R. D'souza[a], Sanket K. Gaonkar[b], Sarvesh S. Harmalkar[a], Pratik A. Asogekar[a], Prof. Irene Furtado[b], Prof. Sunder N. Dhuri[a]*

[a] School of Chemical Sciences, Goa University, Taleigao Plateau, Goa, 403 206 India; *E-mail: sndhuri@unigoa.ac.in*
[b] Department of Microbiology, Goa University, Taleigao Plateau, Goa, 403 206 India

Dedicated to Professor Julio B. Fernandes on the occasion of his 68th birthday

Table of Contents

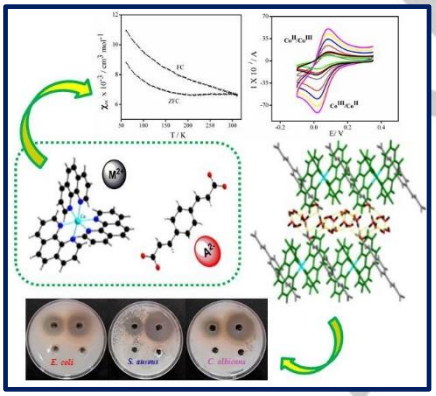

A mononuclear water-rich, Co(II) compound tris-(1,10-phenanthroline)cobalt(II) *p*-phenylenediacrylate tetradecahydrate, $[Co(phen)_3](ppda)\cdot 14H_2O$ (**1**) has been synthesized and characterized by various methods including single crystal X-ray diffractometry. The high spin Co(II) compound has been tested in antibacterial and antifungal activity. The anti-Candida activity of **1** at 100 µg/mL concentration was found to endorse potential as anti-fungal agent.